

PAPER • OPEN ACCESS

The influence of battery degradation level on the selected traction parameters of a light-duty electric vehicle

To cite this article: Z Juda and M Noga 2016 *IOP Conf. Ser.: Mater. Sci. Eng.* **148** 012042

View the [article online](#) for updates and enhancements.

You may also like

- [Diesel passenger vehicle shares influenced COVID-19 changes in urban nitrogen dioxide pollution](#)
Gaige Hunter Kerr, Daniel L Goldberg, K Emma Knowland et al.
- [Review of electrofuel feasibility—prospects for road, ocean, and air transport](#)
Selma Brynolf, Julia Hansson, James E Anderson et al.
- [The role of pickup truck electrification in the decarbonization of light-duty vehicles](#)
Maxwell Woody, Parth Vaishnav, Gregory A Keoleian et al.

ECS Toyota Young Investigator Fellowship



For young professionals and scholars pursuing research in batteries, fuel cells and hydrogen, and future sustainable technologies.

At least one \$50,000 fellowship is available annually.
More than \$1.4 million awarded since 2015!



Application deadline: January 31, 2023

Learn more. Apply today!

The influence of battery degradation level on the selected traction parameters of a light-duty electric vehicle

Z Juda¹ and M Noga¹

¹Institute of Motor Vehicles and Internal Combustion Engines, Cracow University of Technology, 37 Jana Pawla II Avenue, 31-864 Krakow, Poland

email: zjuda@pk.edu.pl; noga@pk.edu.pl

Abstract. The article describes results of an analysis of the impact of degradation level of battery made in lead-acid technology on selected traction parameters of an electric light duty vehicle. Lead-acid batteries are still used in these types of vehicles. They do not require complex systems of performance management and monitoring and are easy to maintaining. Despite the basic disadvantage, which is the low value of energy density, low price is a decisive factor for their use in low-speed electric vehicles. The process of aging of the battery related with an increase in internal resistance of the cells and the loss of electric capacity of the battery was considered. A simplified model of cooperation of the DC electric motor with the battery assuming increased internal resistance was presented. In the paper the results of comparative traction research of the light-duty vehicle equipped with a set of new batteries and set of batteries having a significant degradation level were showed. The analysis of obtained results showed that the correct exploitation of the battery can slow down the processes of degradation and, thus, extend battery life cycle.

1. Introduction

Traction batteries in electric vehicles have a limited lifespan. Battery life depends on many factors, and the end result is the increasing of an internal resistance of a cell and the loss of a battery capacity, which results in limiting the range of the vehicle. Another consequence is a reduction of the stiffness of discharge characteristics, which results in deterioration of operating parameters of the electrical drive. After a long use the degradation processes are accelerated. Another factor degrading the lead-acid battery is also the sulfation of plates of battery cells. The result is a reduction in capacity and increase in internal resistance. Charging of such a battery requires increased charging voltage. Losses of the active material due to mechanical damage reduce the surface of cell plates and also cause a loss of capacity. The objective of the study is to evaluate the effect of degradation processes in a long-term operation in a relation to the important battery parameters such as capacity and the internal resistance of the battery.

2. The object of research and data acquisition path

The research which are the subject of this study were conducted on four-wheeled, light-duty electric vehicle Melex 945 with two seating positions for driver and passenger equipped with a loading platform that allows transport of loads up to 150 kg. The source of propulsion of the vehicle is a separately excited DC motor [1]. Reducing of rotational speed in the drive system is implemented through a two-stage cylindrical gear, which was joined with an electric motor and with a rigid rear



axle suspended on leaf springs. Front suspension is based on transverse-wishbones and a single transverse leaf-spring. Damping of vibrations coming from the road surface roughness is carried out using twin-tube oil shock absorbers located at each wheel. The vehicle uses hydraulic dual-circuit braking system. The fluid pressure produced by the pump acts on the drum brakes of all four wheels. The vehicle also has a set of lighting required to travel on public roads. Basic technical data of the vehicle are shown in Table 1.

Table 1. Basic technical data of the test vehicle

Parameter	Value
Length x width, Wheelbase	2660 x 1230 mm, 1660 mm
Curb weight	700 kg
Load	2 persons + 150 kg load
Motor type	DV3-4006AA, DC, separately excited
Supply voltage	48 V
Armature current	100 A
Nominal motor power	3,9 kW at 4300 rpm
Nominal motor torque	8,2 Nm
Motor efficiency	75%
Overall transmission ratio	16
Maximum speed	29 km/h
Range	About 40 km

2.1. Traction batteries

The electrical energy storage system consist of the 8 lead-acid batteries located in the middle of the vehicle under the driver and passenger seats. Serial connection of batteries with a voltage of 6V each gives the nominal voltage value of 48V for the set. The used batteries are characterized by an increased durability to remain in a state of deep discharge - so called "deep cycle". Technical data of the battery packs used for the tests are shown in Table 2. New batteries have a slightly lower nominal capacity in relation to the previously used traction batteries T-145, and are characterized by a lower mass. The both sets of batteries are of a "deep-cycle" type have thicker plates (the alloy of lead and antimony) and a special type of separator. In turn, the active mass of the plates has a higher density. As a result, the battery life increases. The life of "deep-cycle" battery type declared by the manufacturer in relation to conventional battery shows an increase of nearly 100%.

Table 2. Technical data of energy storage systems used in the tests [2], [3]

Parameter	Old set	New set
Battery type	Trojan T-145, „deep cycle”	Trojan T-125, „deep cycle”
Nominal voltage, V_{bat}	48 V (8x6V)	48 V (8x6V)
Capacity (10h), C_{10}	239 Ah	221 Ah
Stored energy, E_{bat}	11.47 kWh	10.61 kWh
Mass of the battery set, m_{bat}	264 kg	240 kg
Charging system	External charger 230V AC/ 48V 30 A DC	

For the Depth of Discharge (DoD) equal to 20% the Life Cycle reaches 3000 deep charge/discharge cycles. For DoD equal to 50% - Life Cycle is 1200, and for DOD = 100% - Life Cycle is only 600. It should be noted that in real operating conditions the DoD over 80% is not allowed. Reducing of the operating costs caused by increasing of the battery lifetime is mainly related to the extension of time to change the battery pack [4]. Batteries of a "deep-cycle" type are designed for the DoD from 50% to 80%, which qualifies this type of battery for vehicles with purely electric drive. An important factor limiting Life Cycle value is the battery-charging-current in a mode of regenerative braking. High values of the charging current for lead-acid batteries have a degrading impact on the battery plates and the active mass.

2.2. Control system of a motor

Management of the operation of the electric motor is carried out by a programmable electronic control system Curtis 1266 designed to operate with a nominal voltage of 36V or 48V, and a maximum continuous current of the armature of 140A.

The controller is based on the MOSFET technology and adjusts the voltage, the armature- and excitation current by pulse width modulation method (PWM). The frequency of the PWM equals 16 kHz. In the field control subsystem the transistors are connected in a H-bridge circuit [5], so that it was possible to change the polarity of the supply voltage, what allows to change the direction of rotation of the motor. The circuit of the motor armature is powered by the half-bridge transistors, which allows current to flow in both directions to and from the battery, respectively, while the machine works as a motor during acceleration and driving the vehicle at a constant speed and as a generator during regenerative braking. The controller has the ability to change a number of configuration parameters, such as e.g. speed limit, maximum armature- and field current of the motor, and delaying the onset and intensity of the braking process with the recovery of energy to the battery pack. Defining a separate set of controller settings, it is possible for the four driving modes, where the selection is made using two bi-stable switches. Changing the controller settings is carried out using a dedicated programmer Curtis 1311.

2.3. Data acquisition path

To record measured values a portable PC computer and data acquisition card of NI USB-6008 type were used. The data acquisition card has 8 analogue inputs with 12-bit resolution and sampling rate up to 10 kS/s. During the tests the waveforms of voltage V_a and I_a armature current, field current I_f and the pulse signal of motor speed V_s from the Hall sensor were recorded at a frequency of 1 kS/s.

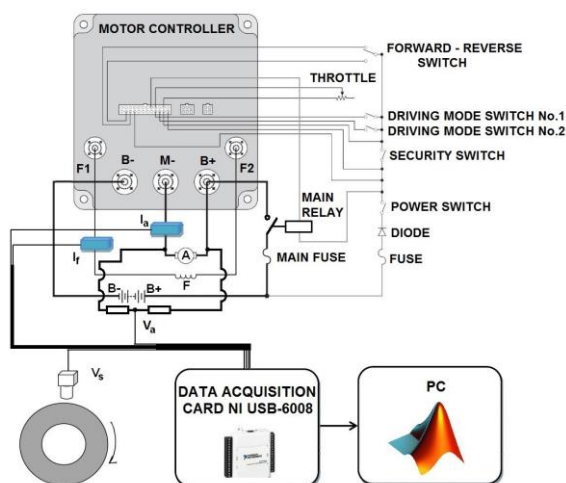


Figure 1. Wiring diagram of the vehicle and scheme of data acquisition path; A - motor armature, F - field wound of the motor, B+, B- - battery connections, M- - negative connection of the motor armature, F1, F2 - connections of the field wound, I_a - sensor of the armature current, I_f - sensor of the field current, V_a - voltage divider for measuring the armature voltage, V_s - sensor of the rotational speed of the motor.

Registration of signals was carried out using a script running in Matlab. The data acquisition path is shown in Figure 1. Besides recording of the voltage signals to the file, the application running in the

Matlab environment allows to convert the stored data to the actual values of the measured parameters. In the case of the armature- and field current measurements, the sensors with Hall effect were used.

Armature voltage is calculated taking into account the ratio of the resistive voltage divider used for measurement, what equals to 6. Application of the divider of voltage armature allows to adjust the level of the measured signal to the input range of data acquisition card.

The modernized system of motor rotational speed measurement, which replaced the original sensor cooperating with the speedometer, was built on the basis of a Hall sensor and a trigger of the motor shaft position made of a ferromagnetic plate. This sensor generates 5 periods of the rectangular signal 0-5V for each revolution of the motor shaft.

The calculation of the speed of the vehicle consisted of counting of falling edges of the rectangular motor speed signal at the time of 200ms using an application developed in MATLAB and converting this indication to the value of speed, taking into account the dynamic radius of the drive wheels and overall transmission ratio. An accurate calibration of the vehicle speed measurement system was performed using a GPS device with a frequency of 100 Hz. In a Figure 2 the courses of vehicle speed obtained from the GPS100Hz-device and newly developed measurement system used in the vehicle were presented. The modernized measurement system allows for the much more precise determination of speed compared to the previously used method.

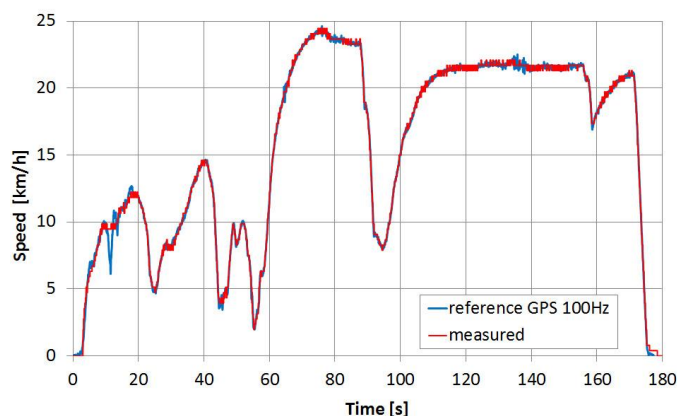


Figure 2. The courses of vehicle speed obtained from the GPS100Hz-device and newly developed measurement system used in the vehicle.

3. Methodology and the scope of research

In September 2015, a set of batteries used since six years in the test vehicle has been replaced by a new one. Batteries used previously have been naturally degrade, which resulted in a drastic reduction of electric capacity and increased internal resistance.

To assess the impact of the application of new batteries on selected traction parameters of Melex vehicle, just before the planned replacement of the battery the research of the vehicle equipped with the old, fully charged, battery pack was carried out. Then, after replacing the batteries with new ones and finished the full charging exactly the same set of tests was performed.

The research of the vehicle was conducted on straight and flat road track with a dry asphalt surface. The test rides to the registration of the results were carried out only in one direction so as to avoid the influence of the inclination of the road on the obtained results. For analogous reasons, during the research the vehicle ran one driver. Before testing, the batteries were fully charged. Vehicle load was about 165 kg (driver, passenger and data acquisition system). Research for both sets of batteries were held in windless and dry weather, at an ambient temperature of 17 °C.

During each of the test runs, after the sudden push the accelerator pedal the vehicle was accelerated to a certain speed, followed by a quick release of the accelerator pedal and the vehicle slowed to a stop with the generator operation of the electric machine and without using the brakes [6]. The vehicle was accelerated to a speed of 26 km/h, which is close to the maximum speed of the vehicle of a fully charged battery pack. This procedure aimed at eliminating the impact of the ongoing battery discharge on the value of maximum speed obtained by the vehicle.

4. The results of research and their analysis

To protect the battery pack and the vehicle electrical circuits against overload the maximum permissible armature current equal to 300A was defined in the motor control system. Due to the short rise time of the voltage to the maximum and the low rotational speed of the motor the armature current reaches the limit value, what sets the controller to a mode of current limiting. This state lasts for about 0.8 seconds and then the motor reaches maximum power. Then the reducing the field current occurs, what allows the motor to operate at a higher rotational speed when adjusting for constant power. This is a classic way to control this type of electrical machines.

4.1. Estimation of characteristic parameters of the two battery sets

An analysis of the obtained results was preceded by estimating of the increase of internal resistance and the actual capacity of the old battery set. The theoretical - experimental method was used for this purpose the details of which will be presented below.

In the first step the internal resistance of a new set of batteries was calculated. For lead-acid batteries the following relationship is true (4.1) [7]:

$$R_{int} = N \cdot \frac{0,022}{C_{10}}, \quad (4.1)$$

where:

R_{int} – internal resistance of the battery, [Ω]

N – number of cells in series connection, -

C_{10} – 10-hour battery capacity, [Ah]

In both cases the number of cells in the battery pack amounts 24, while in the case of a new battery, the 10-hour capacity is 221 Ah. In this situation, an internal resistance of the new battery set is $R_{int_new} = 0.0024$ [Ω].

Estimating the internal resistance of the old set of batteries was based on a comparison of experimental results obtained in similar conditions for both sets of batteries. The comparison was carried out for the first tests of acceleration of the vehicle with fully charged batteries for the both sets of batteries.

An equivalent circuit of the electric drive (Figure 3) was used in order to calculate the resistance of the old battery set. The model of the battery impedance represented only by a real part (resistance) was adopted for this analysis.

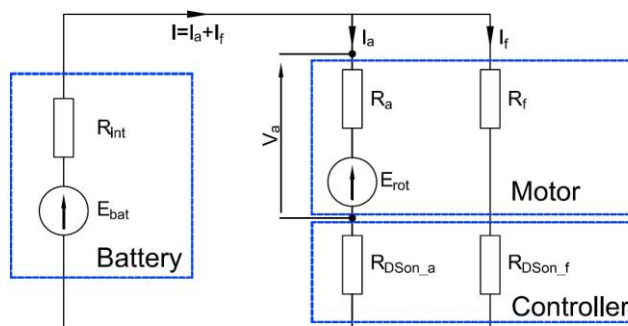


Figure 3. Equivalent circuit of the electric drive.

In the scheme above the following symbols and abbreviations are used:

E_{bat} – electromotive force of the battery, [V]

E_{rot} – electromotive force generated in the armature, [V]

I - current taken from the battery, [A]

I_a – armature current, [A]

I_f – field current, [A]

R_a – armature resistance, [Ω]

R_f – field winding resistance, [Ω]

R_{int} – internal resistance of the battery, [Ω]

$R_{DSon_a/f}$ – on-resistance of MOSFETs in the armature/field circuit of motor controller, [Ω]

V_a – armature voltage, [V]

To determine the internal resistance of the old battery the waveforms of armature current, field current and the voltage measured at the terminals of the armature of the electric motor registered during acceleration of the vehicle with the new and old sets of batteries were analysed.

For a range of speed close to the maximum the same value of the armature current in the waveforms recorded for the both batteries was selected (4.2).

$$I_a = I_{a_old} = I_{a_new} = 96.27 [A], \quad (4.2)$$

The controller provides a flow of field current proportional to the armature current value, what makes that for the both selected points in the waveforms of the armature current the field current also reaches the same values (4.3).

$$I_f = I_{f_old} = I_{f_new} = 8.20 [A], \quad (4.3)$$

Ensuring for both sets of batteries a fully charged state and the same speed of the vehicle causes that the increase in internal resistance of the old battery set is directly proportional to the difference in voltage measured in the analysed conditions on the armature of the motor supplied from new and old batteries, and other circuit parameters remain unchanged. In this case, the internal resistance of the old battery set can be calculated using the formula (4.4).

$$R_{int_old} = R_{int_new} + \frac{V_{a_new} - V_{a_old}}{I_a + I_f}, \quad (4.4)$$

The armature voltage values registered for the new battery set and the old one amount to $I_{a_new} = 48.36$ [V] and $I_{a_old} = 45.72$ [V], respectively, so eventually the estimated value of resistance of the old battery is $R_{int_old} = 0.0277$ [Ω].

Having the calculated value of the internal resistance of the old battery set it is possible to estimate the capacity of the storage system. For this purpose appropriately transformed formula (4.1) was used. Inserting the calculated value of the internal resistance R_{int_old} gives as a result $C_{10_old} = 19.1$ [Ah].

The calculated capacity of the old, exploited battery set is approximately 8% of the original value, what is reflected in the results of research presented in the next section of work.

4.2. Simulation of the behaviour of new and used set of batteries

Simulations were performed using Implement Battery Model from Electrical Sources, Electric Drives / Extra Sources Matlab / SimPowerSystems library [8]. Discharge curves of constant current values 50, 100 and 150 A show the characteristics of rigidity to the entire area of the battery not showing signs of wear – Figure 4, and large voltage drops to the exploited battery, what is clearly visible in the Figure 5.

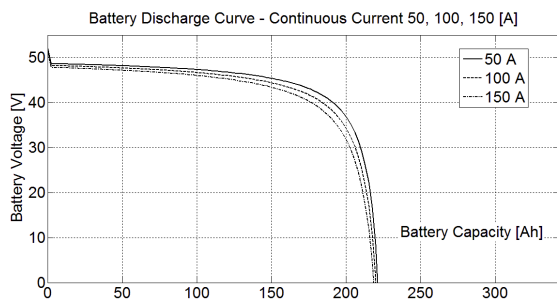


Figure 4. Battery discharge curve – capacity 220 Ah – new set.

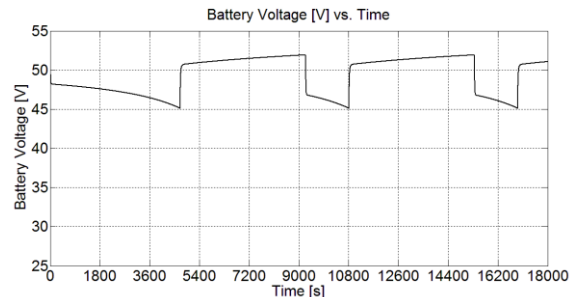


Figure 5. Battery discharge curve – capacity after degradation - 20Ah.

Figure 6 shows the result of simulation of a constant current discharging the battery 100 A from the state of full charge (SOC = 1) to SOC = 0.4, and constant current charging to achieve the SOC value = 0.6. Discharge of the battery is made within 1.31 hour. Recharging to the SOC = 0.6 required a time of 1.26 hour. Additional discharged to the SOC = 0.4 occurred after 0.43 hour. During the process of charging and discharging a terminal voltage of the battery has changed in the range of 45.12 V to 51.93 V.

A similar process for the exploited battery – Figure 7 - showed different behaviour under identical conditions. Battery discharge occurred after the time of 8.55 min. and to recharge to the SOC = 0.6 time 9.51 min was needed. Another discharged to the SOC = 0.4 occurred at 2.65 min. In the process of charging and discharging terminal voltage of the battery has changed in the range of from 27.99 V to 55.27 V.

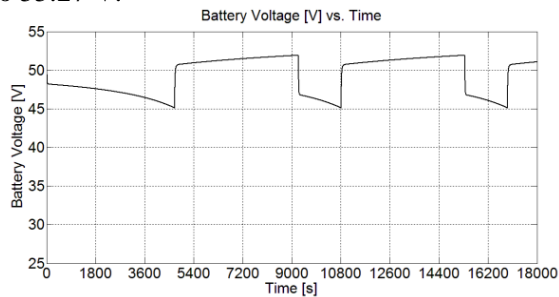


Figure 6. Battery voltage during charging/ discharging – 220 Ah – new set.

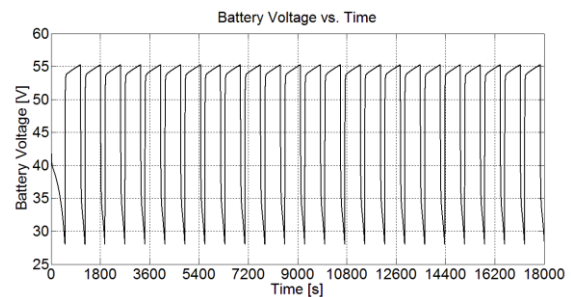


Figure 7. Battery voltage during charging/ discharging – 20 Ah – after degradation.

The loss of battery capacity due to progressive degradation leads to faster discharge, thus increasing the frequency of charge / discharge cycle which has a direct impact on battery life [9].

4.3. Selected issues of the process of acceleration of the electric vehicle with new and old energy storage systems

Figure 8 presents a comparison of the maximum power taken from the battery pack during the process of acceleration of the electric vehicle with the old and new set of batteries as a function of the parameter Acceleration rate, i.e. the elapsed time of increasing of the armature voltage from zero to the maximum value.

Analysis of the content of Figure 8 indicates that the course of changes of maximum power taken from battery is similar in nature for the new and old batteries. Lower values obtained for the old batteries are the result of the increased voltage drop across the internal resistance of the battery, which increases with the degree of discharge of battery and with its degradation.

Figure 9 shows a comparison of the maximum armature current registered in the same conditions as before. The maximum values of the armature current obtained for successive values of the parameter Acceleration rate are practically the same for both sets of batteries. This is due to the fact that the controller enters in the phase of current limitation when starting the motor regardless of the state of the battery. This is caused by low armature resistance and the low value of the electromotive force induced in the rotor at a low rotational speed.

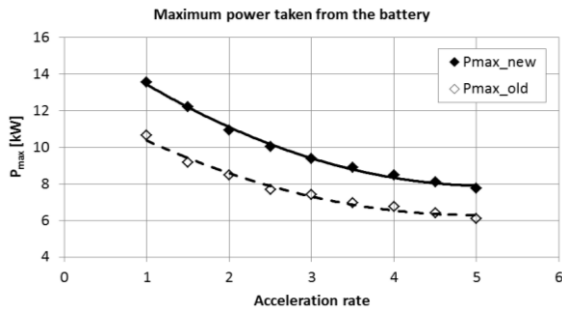


Figure 8. The maximum power taken from the battery during acceleration of the electric vehicle with the old (Pmax_old) and new (Pmax_new) set of batteries as a function of Acceleration rate.

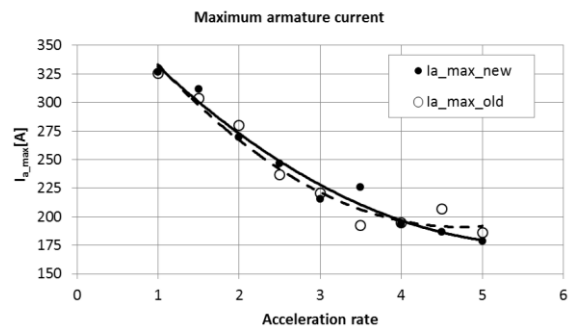


Figure 9. The maximum armature current during acceleration of the electric vehicle with the old and new set of batteries as a function of Acceleration rate.

The maximum value of the voltage measured at the motor armature is observed when the vehicle reaches maximum speed. This value depends directly on the internal resistance of the battery. Figure 10 shows the maximum armature voltage recorded in the successive tests for the both sets of batteries.

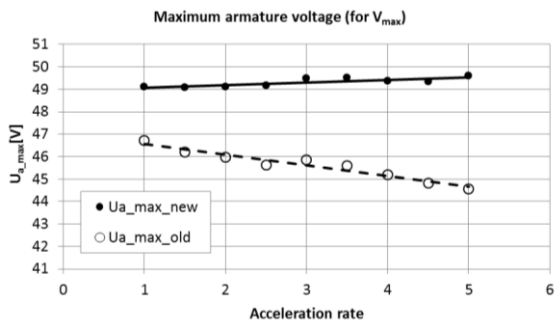


Figure 10. The maximum armature voltage as a function of Acceleration rate for the both set of batteries.

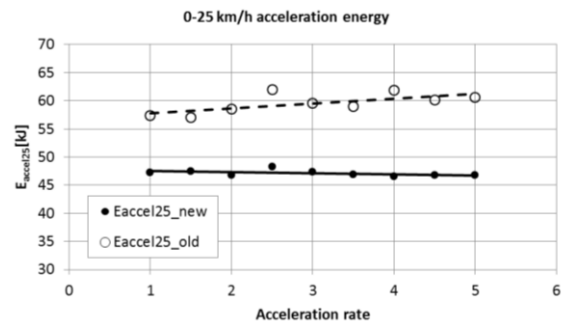


Figure 11. Electric energy taken from the battery pack during acceleration of the vehicle to a speed of 25 km/h for different values of the parameter Acceleration rate.

The maximum value of the armature voltage in the terms of measurements represents the condition of the battery pack. A curve with a slightly increasing trend in subsequent tests was obtained for the set of new batteries. This phenomenon can be explained by the fact that in subsequent attempts the time of voltage rise to the nominal value was gradually increasing, what gave lower values of armature current observed in the first phase of acceleration. If so, the lower load of the power supply resulted in lower voltage drop during the first phase of acceleration. In this situation the armature voltage at the end of acceleration reached gradually increasing values. In the successive tests significantly decreasing maximum values of the armature voltage were obtained for the set of old batteries. This is due to a very rapid process of discharging of the old batteries caused by their sulfation what lowers electric capacity.

The dependence of electric energy taken from the battery pack during acceleration of the vehicle to a speed of 25 km/h for different values of the parameter Acceleration rate is presented in Figure 11. For the new set of batteries the energy of the vehicle acceleration to desired speed is practically independent on the intensity of the first phase of the process of acceleration. For the old battery set, the energy of acceleration is significantly higher than for the new battery set - to about 25%. In addition, the energy rises in the successive test drives. This results from the large energy losses on the increased

internal resistance of the old battery set, additionally increasing in subsequent test drives, as described above.

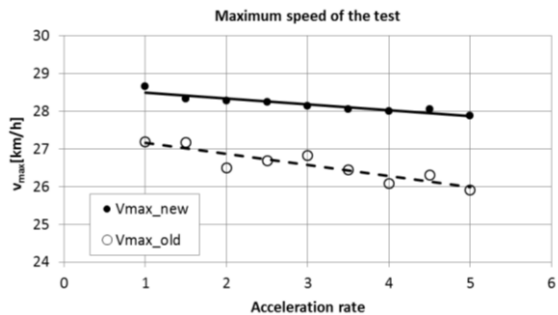


Figure 12. Maximum speed reached in the test track as a function of the parameter Acceleration rate.

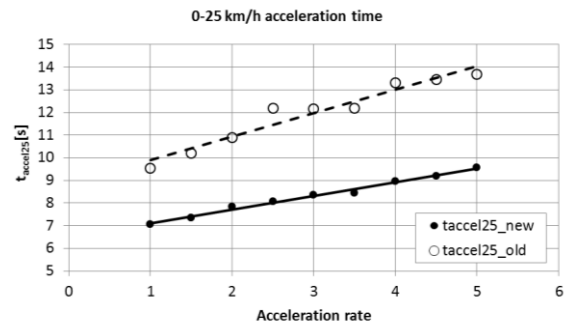


Figure 13. Time of acceleration to a speed of 25 km/h as a function of the parameter Acceleration rate obtained for the vehicle fitted with a set of old and new batteries.

A graph of the maximum speed of the vehicle obtained on the length of the test track is shown in Figure 12. For the both battery sets new and old the maximum speed decreases with increasing value of the parameter Acceleration rate. This is caused by the fact that the acceleration takes place all the time on the track of the same length, so if accelerating is milder, the speed obtained by the vehicle will have a gradually decreasing value. In the case of old set of batteries this effect is compounded by a gradual discharge of the battery, what, as mentioned above, can be seen analysing the successive test results.

Graphs of time of acceleration to a speed of 25 km/h as a function of the parameter Acceleration rate obtained for the vehicle fitted with a set of old and new batteries were presented in Figure 13. The acceleration time of the vehicle to a speed of 25 km/h depending on the intensity of increase of the voltage to the maximum value is rising in both cases. For the new set of the batteries the time is increased from about 7 seconds for the Acceleration rate equalled 1.0 s to about 9.5 s for the setting Acceleration rate = 5.0 s. For the old set of batteries, the values being 9.5 and 13.8 s, respectively, what indicates a significant decrease in maximum performance of the vehicle.

Figure 14 shows waveforms of changes in the value of the average acceleration to a speed of 25 km/h depending on the value of Acceleration rate parameter obtained for the vehicle fitted with a set of new and old batteries.

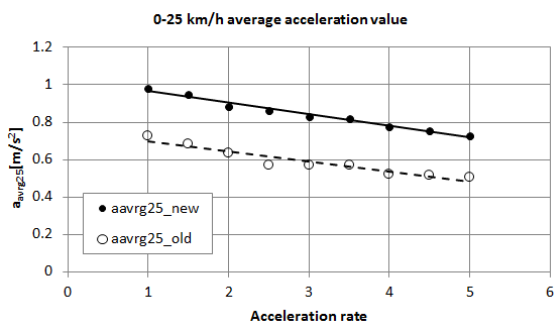


Figure 14. The average acceleration to a speed of 25 km/h depending on the value of Acceleration rate parameter obtained for the vehicle fitted with a set of new and old batteries.

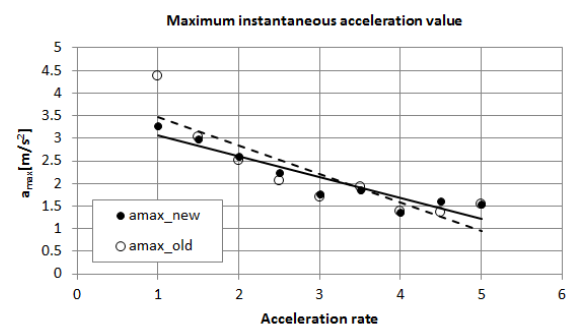


Figure 15. The maximum instantaneous acceleration of the vehicle in a function of Acceleration rate parameter for the vehicle with the old and new battery pack.

The curves of changes in the value of the average acceleration to a speed of 25 km/h are inverted to the waveforms of acceleration time shown in the previous figure. Figure 15 shows a comparison of the maximum instantaneous acceleration of the vehicle in a function of Acceleration rate parameter for the vehicle with the old and new battery pack. The maximum instantaneous acceleration value is recorded in the first phase of acceleration of the vehicle from a standing start. The acceleration depends on the torque to the wheels of the vehicle, and in turn, this value is derived from the torque of the motor which is directly proportional to the armature current. It should be remembered that the maximum value of the armature current in both cases was similar. If so, the instantaneous maximum torque underlying the maximum acceleration of the vehicle will obtain similar waveforms, regardless of the state of charge of the battery in the vehicle.

5. Conclusions

Basing on the results of carried out research described in the paper, the following conclusions were formulated:

- In the case of electric drive the intensity of the process of acceleration to the desired speed has no significant impact on energy consumption,
- The operation of an electric vehicle with a worn out battery pack is associated with a drastic deterioration of performance, such as maximum speed, acceleration and most of all range,
- Increased internal resistance of the battery exhibiting a high degree of wear causes high energy losses, in the case of the test vehicle. This value reached a level of about 25%. In the same way drops the overall efficiency of the electric power source,
- The relationship similar to the above mentioned will be valid also in the process of charging of the worn out batteries. A part of the energy provided by a rectifier will dissipate to the heat on the internal resistance of individual cells,
- The efficiency of the recovery of kinetic energy in the process of regenerative braking will decrease for the same reasons in the case of operation with worn out batteries.

Acknowledgements

Authors would like to thank Dr. Robert Janczur for the lending of the 100Hz GPS device used to calibrate speed measurement system.

References

- [1] Khajepour A, Fallah S and Goodarzi A 2014 *Electric and Hybrid Vehicles* (Chichester: John Wiley & Sons)
- [2] Trojan T-145 Battery Data Sheet 2015 (Santa Fe Springs: Trojan Battery Company)
- [3] Guo J, Wang J and Cao B 2009 *Regenerative Braking Strategy for Electric Vehicles* Intelligent Vehicles Symposium (Xi'an: IEEE) p 864-868
- [4] Eshani M, Gao Y, Gay S E and Emadi A 2005 *Modern Electric, Hybrid Electric and Fuel Cell Vehicles, Fundamentals, Theory and Design* (Boca Raton: CRC Press)
- [5] Trojan T-125 Battery Data Sheet 2016 (Santa Fe Springs: Trojan Battery Company)
- [6] Juda Z 2014 *Hamowanie odzyskowe pojazdów z napędem elektrycznym – strategię sprawności odzysku i komfortu jazdy* Badania Pojazdów (Cracow: Politechnika Krakowska) p 49-60
- [7] Larminie J and Lowry J 2003 *Electric Vehicle Technology Explained* (Chichester: John Wiley & Sons)
- [8] Tremblay O, Dessaint L A and Dekkiche A I 2007 *A Generic Battery Model for the Dynamic Simulation of Hybrid Electric Vehicles*, IEEE Vehicle Power and Propulsion Conference, (Arlington: IEEE)
- [9] Juda Z 2001 *Simulation of Energy Conversion in Advanced Automotive Vehicles* SAE Technical Paper 2001-01-3341, (Warrendale: SAE)